Longitudinal coherence function in X-ray imaging of crystals

Steven J. Leake,[1,*] Marcus C. Newton,[1] Ross Harder,[2] and Ian K. Robinson[1,3]

[1]*London Centre for Nanotechnology, University College, Gower St, London WC1E 6BT, UK*
[2]*Argonne National Laboratory, 9700 South Cass Avenue, Argonne, IL 60439, USA*
[3]*Diamond Light Source, Harwell Campus, Didcot, OX11 0DE, UK*
** s.leake@ucl.ac.uk*

Abstract: The longitudinal coherence function at the Advanced Photon Source beamline 34-ID-C has been measured by a novel method and the coherence length (ξ_L) determined to be, $\xi_L = 0.66 \pm 0.02\mu m$. Three dimensional Coherent X-ray Diffraction (CXD) patterns were measured for multiple Bragg reflections from two Zinc Oxide (ZnO) nanorods with differing aspect ratios. The visibility of fringes corresponding to the 002 crystal direction for each reflection were found to be different and used to map the coherence function of the incident radiation. Partial coherence was found to be associated with amplitude 'hot' spots in three dimensional reconstructions of the crystal structure.

OCIS codes: (030.1640) Coherence; (110.7440) X-ray imaging; (100.5070) Phase retrieval

References and Links

1. I. A. Vartanyants, and I. K. Robinson, "Partial coherence effects on the imaging of small crystals using Coherent X-ray Diffraction," J. Phys. Condens. Matter **13**(47), 10593–10611 (2001).
2. G. Grübel, and F. Zontone, "Correlation spectroscopy with coherent X-rays," J. Alloy. Comp. **362**(1-2), 1–2, 3–11 (2004).
3. S. G. J. Mochrie, L. B. Lurio, A. Ruhm, D. Lumma, M. Borthwick, P. Falus, H. J. Kim, J. K. Basu, J. Lal, and S. K. Sinha, "X-ray photon correlation spectroscopy studies of colloidal diffusion and the capillary modes of polymer films," Physica B **336**(1-2), 173–180 (2003).
4. B. Lengeler, "Coherence in X-ray physics," Nature **88**(6), 249–260 (2001).
5. F. Livet, "Diffraction with a coherent X-ray beam: dynamics and imaging," Acta Crystallogr. A **63**(2), 87–107 (2007).
6. I. K. Robinson, C. A. Kenney-Benson, and I. A. Vartaniants, "Sources of decoherence in beamline optics," Physica B **336**(1-2), 56–62 (2003).
7. D. Sayre, "Some implications of a theorem due to Shannon," Acta Crystallogr. **5**(6), 843 (1952).
8. J. R. Fienup, "Reconstructions of an object from the modulus of its Fourier transform," Opt. Lett. **3**(1), 27–29 (1978).
9. G. J. Williams, M. A. Pfeifer, I. A. Vartanyants, and I. K. Robinson, "Internal structure in small Au crystals resolved by three-dimensional inversion of coherent x-ray diffraction," Phys. Rev. B **73**(9), 094112 (2006).
10. M. A. Pfeifer, G. J. Williams, I. A. Vartanyants, R. Harder, and I. K. Robinson, "Three-dimensional mapping of a deformation field inside a Nanocrystal," Nature **42**(7098), 63–66 (2006).
11. S. Marchesini, "Invited article: a [corrected] unified evaluation of iterative projection algorithms for phase retrieval," Rev. Sci. Instrum. **78**(1), 011301 (2007).
12. M. Born, and E. Wolf, *Principles of Optics*, (Cambridge University Press, 1999), Chap. 10.
13. F. Veen, and F. Pfeiffer, "Coherent x-ray scattering," J. Phys. Condens. Matter **16**(28), 5003–5030 (2004).
14. J. Als-Nielsen, and D. McMorrow, *Elements of Modern X-ray Physics*, (John Wiley & Sons, 2001).
15. M. Newton, S. Firth, T. Matsuura, and P. Warburton, "Synthesis and characterization of zinc oxide tetrapod nanocrystals," J. Phys. Conf. Ser. **26**, 251–255 (2006).
16. M. A. Pfeiffer, *PhD thesis*, University of Illinois (2005).
17. R. Harder, M. A. Pfeifer, G. J. Williams, I. A. Vartaniants, and I. K. Robinson, "Orientation variation of surface strain," Phys. Rev. B **76**(11), 115425 (2007).
18. W. L. Bragg, "The diffraction of short electromagnetic waves by a crystal," Proc. Camb. Philos. Soc. **17**, 43–57 (1913).
19. A. I. Chumakov, A. Q. R. Baron, R. Rüffer, H. Grünsteudel, H. F. Grünsteudel, and A. Meyer, "Nuclear resonance energy analysis of inelastic x-ray scattering," Phys. Rev. Lett. **76**(22), 4258–4261 (1996).

#111397 - $15.00 USD Received 14 May 2009; revised 18 Jun 2009; accepted 19 Jun 2009; published 21 Aug 2009

1. Introduction

The mutual coherence of an electromagnetic wave is defined as the two-point correlation function of its electric field. It is normally measured as the visibility of a fringe system in a suitable interferometer. Interferometric measurements can be difficult to achieve for hard X-rays because of the small length scales involved, yet knowledge of the coherence properties is vital for some of the newest imaging techniques being explored at third-generation sources of Synchrotron Radiation (SR).

In this letter, we report that the visibility of the diffraction fringes due to interference between the ends of an extended object carries the same information about the coherence of the illuminating wavefield as the classical double-slit interferometer. This neatly overcomes the practical problem of cutting out two sample points in a wave field separated by a distance of the order of a micron. We show how to exploit this visibility to measure the longitudinal coherence. Advances in experimental design allowed us to measure the same fringe system for multiple Bragg peaks from the same micron-sized crystal. In this way the full longitudinal coherence function has been mapped out using just two crystals.

2. Coherent X-ray Diffraction

Coherent X-ray Diffraction (CXD) imaging in the Bragg geometry is sensitive to lattice distortions with sub angstrom sensitivity. CXD is becoming an important technique for the study of defects within, and properties of, surfaces and interfaces of nanocrystalline materials [1]. Akin to other forms of coherence based experiments such as X-ray Photon Correlation Spectroscopy and Phase Contrast imaging, CXD is vitally dependent on the coherence properties of the illuminating radiation [2–6].

CXD imaging is feasible only when the entire illuminated volume of a crystal is within a coherent beam of X-rays. Scattering from the entire volume of the crystal will interfere at each Bragg reflection producing a three-dimensional continuous diffraction pattern. The scattered amplitude is a complex quantity, $A = |A|\exp(i\varphi)$, the Fourier Transform of which is the three-dimensional electron density of the illuminated crystal. In direct space, the phase (φ) of the complex density describes the displacement of the crystal planes parallel to the Q-vector, $\varphi = \vec{Q}.\vec{r}$. The Q-vector remains approximately constant for the measurement thus CXD is sensitive to displacements of the crystal planes. Only the intensities ($I = |A|^2$) of the continuous diffraction pattern are measured using an area detector, however, giving rise to a `Phase Problem'. To recover the phases of the measured moduli the diffraction pattern must be sampled at greater than the Nyquist frequency for the size of the crystal [7]. Using a Hybrid Input Output (HIO) algorithm with a support constraint is usually sufficient to find a set of phases consistent with the measured amplitude [8]. This algorithm has been employed to recover three dimensional images from a single Bragg reflection of a gold nanocrystal [9] and a lead nanocrystal [10]. An excellent review of the phasing algorithms has been provided by Marchesini [11].

3. Coherence

The coherence properties of the illuminating radiation are quantified by the complex degree of coherence, γ_{12} [12], describing the normalised correlation between points 1 and 2 in an electromagnetic field. Its magnitude $|\gamma_{12}|$ is measurable as the visibility of a fringe system generated by an two slit interferometer (Young's double slit experiment) for the lateral coherence:

$$V = \frac{I_{\max} - I_{\min}}{I_{\max} + I_{\min}} \tag{1}$$

#111397 - $15.00 USD Received 14 May 2009; revised 18 Jun 2009; accepted 19 Jun 2009; published 21 Aug 2009

Where I_{max}/I_{min} are the fringe maxima/minima intensities. This gives rise to three regimes; coherent, $\gamma_{12} = 1$, partially coherent, $0 < |\gamma_{12}| < 1$ and incoherent, $\gamma_{12} = 0$. Young's double slit experiment considers the simplistic interference between two point scatterers (i.e ideal pinholes). Here, instead, we consider partially coherent illumination of a uniform material with clean cut ends (a nanocrystal). The intensity distribution I(y) observed across a detector as a function of position *y* on a detector at a distance *D* from the crystal can be expressed as:

$$I(y) = I_0 \int_{-a/2}^{a/2} (a - |x|)\gamma(x) \exp(\frac{ikyx}{D}) dx \qquad (2)$$

Here, I_0 is proportional to the square of the incident wave amplitude and the density of the illuminated crystal, $\gamma(x)$ is equal to γ_{12} for two points separated by *x*, *a* is the dimension of the crystal between clean cut ends and *k* the wavenumber. The visibility of the function I(y) in Eq. (2) can be demonstrated to be numerically equal to the magnitude of γ, the mutual coherence along the length of the crystal, at least for a gaussian form of $\gamma(x)$.

The coherence of a beam of light, including undulator X-ray beams, is often discussed as having two components, both transverse and longitudinal coherence lengths, ξ_T and ξ_L respectively [13,14]. The transverse coherence is dependent on the source itself. A synchrotron source consists of incoherent emitters confined to a distribution in space of width σ. Two points within the sample will see the source with the same relative phase up to a separation distance $\xi_T = \lambda D/2\sigma$, where D is the distance from the source to the sample. The longitudinal coherence is dependent on the bandwidth of the monochromator ($\Delta\lambda/\lambda$) attributed to the apparent thickness of the monochromator crystal via its Darwin width, $\xi_L = \lambda^2/2\Delta\lambda$. This couples to the Optical Path Length Difference (OPLD) of rays through the sample. When the OPLD is smaller than ξ_L the sample is said to be in the coherent limit and meets the required conditions for CXD measurements. For a typical synchrotron source; ξ_T = 10µm in the horizontal, ξ_T = 50µm vertical and ξ_L < = 0.7µm for a Silicon (111) monochromator. The fringe visibility can be lost by violation of any of the three coherence requirements and is only present if all three are satisfied. In our experiment V is limited by ξ_L so the transverse coherence will not be discussed further.

4. Methods

Novel sample preparation methods were needed to fiducialise the samples so that multiple Bragg peaks could be measured from the same crystal. Zinc Oxide (ZnO) rods were synthesised using the Chemical Vapour Transport (CVT) method [15] of the order 1-2µm in diameter and 2-6µm in length. Scanning Electron Micrographs (SEM) show a flat ended prism morphology, i.e rod. Si (001) substrates were diced into 10x10mm and a cross scored through the centre of each die. An individual ZnO rod was placed in a marked corner quadrant as close to the centre as possible using a micromanipulator; Van der Waals forces attract a chosen nanorod to the manipulation probe, contact with the surface being sufficient to deposit the rod on a Si wafer substrate in a marked location. Samples were then annealed in O_2 at 950°C for 1 hour to grow the SiO_2 layer by approximately 50nm anchoring the crystals to the substrate.

Coherent diffraction measurements were conducted at 34-ID-C beamline at the Advanced Photon Source, Argonne National Laboratory. The beamline consists of an undulator set to 9keV, a beam splitting mirror directs the beam onto a silicon double crystal monochromator and a set of roller blade slits define the beam dimensions in the horizontal and vertical direction (10-100µm). The sample was mounted on translation stages and then moved into the beam, using the scored pattern as an identifying marker. A stationary CCD detector was used to sample the diffraction pattern; 2-dimensional slices were recorded as the Bragg peak was rocked through the detector by rotating the sample in the beam. Slices were stacked into a 3D reciprocal lattice map of each peak using an appropriate coordinate transformation [16,17].

#111397 - $15.00 USD Received 14 May 2009; revised 18 Jun 2009; accepted 19 Jun 2009; published 21 Aug 2009

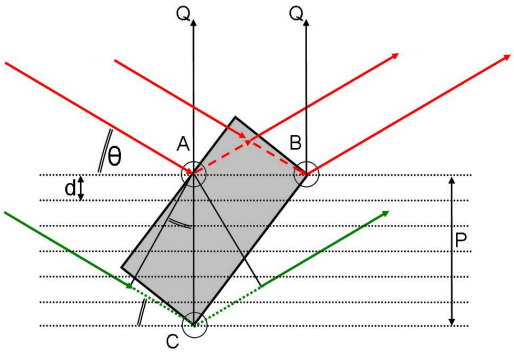

Fig. 1. Schematic of diffraction from point scatters A,B and C for OPLD calculation; $OPLD_{AB} = 0$, $OPLD_{AC} = 2BC\sin\theta$

Figure 1 shows a crystal (grey rectangle) illuminated at the angle satisfying Braggs Law for a set of lattice planes that correspond to the reciprocal lattice vector Q. The OPLD between two coherent x-rays scattering from points within the same plane (A and B) will be zero, hence the longitudinal coherence is independent to the length of the crystal perpendicular to the Q-vector. If two scatterers (B and C) are positioned at the extreme extents of the crystal, the OPLD (dotted line through point C) in this scenario is simply the product of the plane layer spacing *d* with the number of planes between the two scattering points with an additional angular (θ) scaling given by Braggs law [18]. This length equates to the projection of the long axis of the crystal onto the Q-vector and is therefore the maximum OPLD of the measurement. Hence, measurement of a finite crystal in the Bragg geometry using CXD is viable if the longitudinal coherence is greater than the projection of each of the crystals dimensions onto the Q-vector. If the inequality is violated the fringes will become less visible in, at least, that direction.

5. Experiments

Multiple values of the OPLD can now be probed for a given crystal by the simple expedient varying Q by observing multiple Bragg peaks. The visibility of the same c-axis can be compared among these measurements. Five Bragg peaks from the first ZnO nanocrystal were measured; diffraction data were sampled by extracting a line of points through the measured distribution of the Bragg peak oriented along the 002 crystal direction in reciprocal space. The results for the 5 Bragg reflections are shown in Fig. 2.

#111397 - $15.00 USD Received 14 May 2009; revised 18 Jun 2009; accepted 19 Jun 2009; published 21 Aug 2009

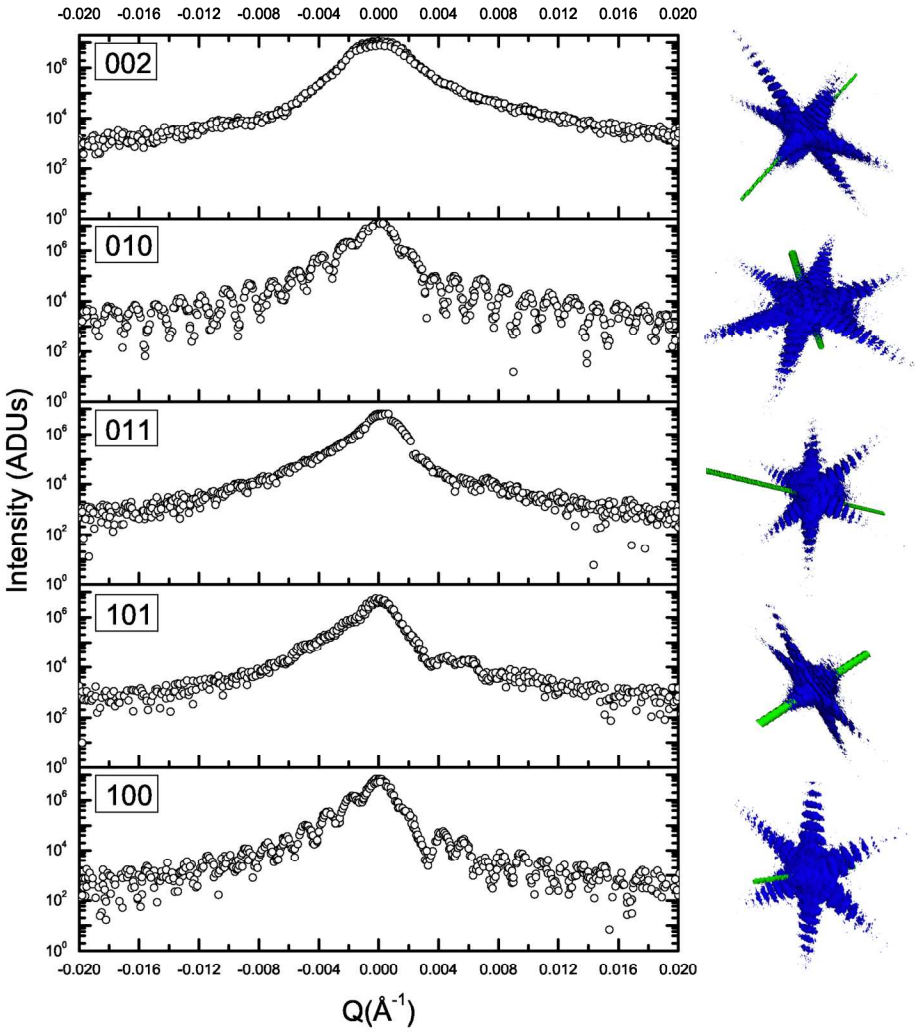

Fig. 2. Measured intensity as a function of momentum transfer deviation along the 002 crystal direction (reciprocal space) demonstrating the 002 fringe visibility for 5 different Bragg peaks from the first ZnO nanocrystal (Left), Corresponding 3D render of diffraction data and line of sampled points (Right)

The fringes are clearly visible in the 100 and 010 reflection, less visible for 101 and 011 and not visible for the 002. We fit Lorentzian functions to the maxima and minima of the fringes to obtain the visibility. The decrease in fringe visibility as a function of the projection of the crystals c-axis along the Q-vector allows us to map out the coherence function of the source. Figure 3 shows these data combined with 11 additional Bragg reflections from a second ZnO crystal with different aspect ratio (1μm x 1.6μm). A Gaussian function fitted to the coherence function has a Half Width Half Maximum (HWHM) of 0.66 ± 0.02μm, we take this width as an estimate of ξ_L it implies a wavelength spread; $\Delta\lambda/\lambda = 1.07\text{x}10^{-4} \pm 0.16\text{x}10^{-4}$ and is within the expected range ($1.0\text{-}2.9\text{x}10^{-4}$) for a Si(111) monochromator at 9keV [14,19].

#111397 - $15.00 USD Received 14 May 2009; revised 18 Jun 2009; accepted 19 Jun 2009; published 21 Aug 2009

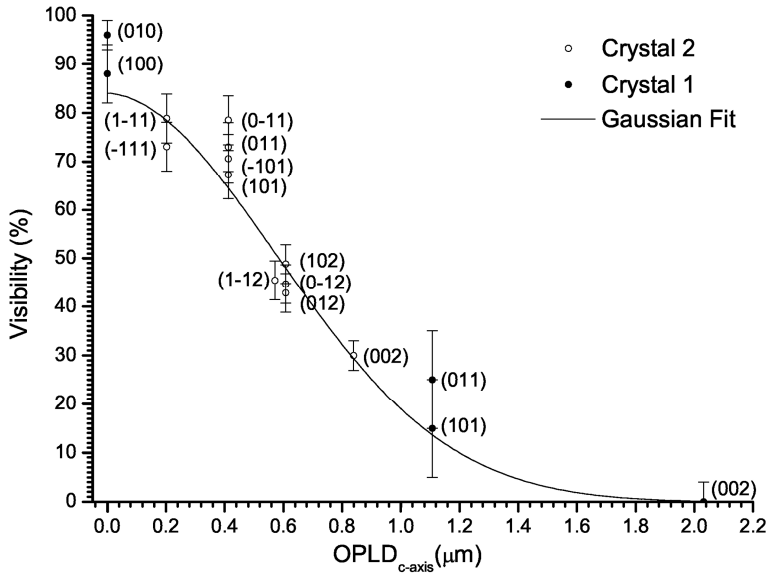

Fig. 3. Visibility as a function of OPLD for 16 Bragg reflections measured from 2 separate ZnO crystals.

The affect of a partially coherent illumination on the ability of the phasing algorithms to reconstruct the electron density was investigated. The image reconstructions of both 010 and 101 reflections of crystal 1 are shown in Fig. 4, the raw data possess visibilities of 96 ± 3% and 25 ± 10% representing both the fully coherent (010) and partially coherent (101) geometries. The coherent 010 reconstruction has well defined facets with a uniform amplitude distribution and the region of low amplitude in the bottom right corner was attributed to a strained region of the crystal. The partially coherent 101 reconstruction has one well defined facet and one rough end and is an incorrect solution for the diffraction data. The spacing of interference fringes defines the size of the object and the number of fringes defines the resolution of the image obtained. When this information has been smeared out by a lack of coherence, the phasing algorithm seeks a solution which would mimic this behavior. Practically, this could manifest as a crystal with two facets along the direction of interest, one flat and the other rough.

Scanning Electron Micrographs and fully coherent Bragg reflections confirmed the crystal size for the two reflections to be 4.08μm x 1.10μm. In the 010 case the reconstruction accurately reproduced the crystal dimensions and in the 101 case the reconstruction was less than half the size of the actual crystal (2μm) with the high amplitude region superimposed on a lower amplitude correct representation of the crystal. Features of this type were coined 'hot' spots and were first predicted [1], and observed in 2D reconstructions from Au nanocrystals [9]. As the fringe visibility drops, the algorithm finds a superposition solution of a low amplitude fringe pattern and high amplitude fringeless pattern creating a 'double image'; this appears in direct space as a low amplitude full size representation of the object and a superimposed, foreshortened 'hot' spot.

#111397 - $15.00 USD Received 14 May 2009; revised 18 Jun 2009; accepted 19 Jun 2009; published 21 Aug 2009

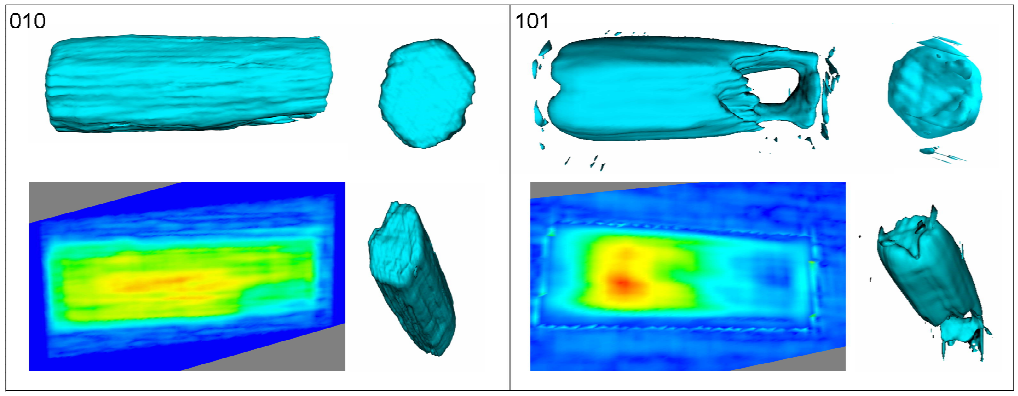

Fig. 4. Corresponding isosurface and scalar cut planes of the reconstructed density of crystal 1 using diffraction data surrounding the 010 and 101 Bragg reflections, as labeled.

6. Conclusion

We have shown that the longitudinal coherence length can be determined by measuring the visibility of the fringe system (generated by the illumination of a finite crystal with x-rays) relative to the projection of the corresponding dimension onto the Q-vector. At the Advanced Photon Source (APS) 34-ID-C beamline the longitudinal coherence was measured to be, ξ_L = 0.66 ± 0.02μm. The phase retrieval from partially coherent Bragg reflections were compromised by the visibility of the observed fringe pattern. False solutions resulted and led to features in the reconstructions such as 'hot' spots of amplitude and combinations of well defined and rough facets deemed incorrect by the reconstructions from the fully coherent geometries. This will have consequences for thin film characterization methods, films with a thickness close to the longitudinal coherence in the specular geometry will observe smearing in the non-specular reflections (depending on the size of the beam footprint and penetration depth). Our work confirms the notion that it is vital to know the coherence lengths of the incident radiation and ensure they are larger than the OPLD for any measured Bragg reflection. This confirms that any smearing present in the diffraction pattern is a property of the crystal alone, i.e. due to internal strains.

Acknowledgements

This work was supported by EPSRC Grant No. EP/D052939/1. The experimental work was carried out at APS beamline 34-ID-C, built with funds from the US National Science Foundation under grant DMR-9724294 and operated by the U.S. Department of Energy, Office of Science, Office of Basic Energy Sciences, under Contract No. DE-AC02-06CH11357.

#111397 - $15.00 USD Received 14 May 2009; revised 18 Jun 2009; accepted 19 Jun 2009; published 21 Aug 2009